Dynamics of a Vicsek fractal: The boundary effect and the interplay among the local symmetry, the self-similarity, and the structure of the fractal

C. S. Jayanthi and S. Y. Wu

Department of Physics, University of Louisville, Louisville, Kentucky 40292
(Received 24 September 1993; revised manuscript received 21 March 1994)

The role of the boundary condition on the transverse vibrations of an nth-stage Vicsek fractal as $n \to \infty$ was studied using nearest-neighbor interactions. Our findings indicate that, although the interplay among the local symmetry, the self-similarity, and the structure is the underlying reason for the unusual properties of the Vicsek fractal, the boundary condition has definitely left its imprint on almost every feature of the dynamics of the system.

I. INTRODUCTION

In the last decade, studies on the properties of complex systems have demonstrated that the concept of fractal may serve as a common link to represent complicated phenomena in diverse scientific disciplines.[1] This realization has generated a concerted effort to understand the eigenvalue spectrum and the eigenstates of fractal structures. The results of these studies have uncovered many unusual features, including the existence of anomalous density of states[2,3] and the superlocalization of some eigenstates.[4-6] However, because of the difficulties associated with an appropriate description of the local properties of the eigenstates in terms of some smooth function, there is yet no proper prescription to define and determine the characteristic length of the eigenstates on random fractals. On the other hand, the prospect of obtaining an exact solution to the eigenvalue problem of some standard fractals prompted the studies on nonrandom fractals. It turned out that these fractals possess unusual and exotic features of their own. In a detailed analysis of the dynamics of a Sierpinski gasket,[7] Rammal found that the frequency spectrum of a Sierpinski gasket is composed of two distinct pure point spectra; one composed of "molecular" modes with nonvanishing amplitudes only at a set of finite sites and other composed of "hierarchical" modes with nonvanishing amplitudes only inside a triangle surrounding a given hole in the gasket. Recently, in a series of papers, we studied the dynamics of a Vicsek fractal.[8-10] The Vicsek fractal is a treelike structure. It differs from the Sierpinski gasket in that it is a loopless structure. Any branch of the Vicsek fractal can be severed from the main body by simply cutting one connecting bond. Using renormalization-group approach, You *et al.* have also studied the electronic and vibrational properties of the Vicsek fractal.[11] In particular, they show that the average density of states consists of hierarchies of isolated peaks following elegant recursive structural rules.

In our earlier study, we had investigated the transverse vibrations of the Vicsek fractal for the fixed-end boundary condition using nearest-neighbor interactions.[9,10] One of the outstanding features of the eigenfrequency spectrum was that a threefold degenerate mode, once it

emerged repeated itself at the same eigenfrequency in all the subsequent stages while its degree of degeneracy increased from a given stage to the next. We had referred such modes as persistent modes in our earlier papers. In Ref. 9, we had used an analysis based on local symmetry and self-similarity to characterize the degenerate and the nondegenerate components of the frequency spectrum, the origin of the persistent degenerate modes, and the general pattern of evolution of the frequency spectrum from a given stage to the next. This analysis led to an exact calculation of the vibrational density of states (DOS) of the Vicsek fractal as $n \to \infty$, where an approach similar to the decimation technique was used.[10] The results of these calculations demonstrated that the frequency spectrum of the Vicsek fractal was very unusual. It had highly degenerate atomiclike levels superimposed on a cantorlike, point dense background. The persistent degenerate modes were all found to be superlocalized, while the nondegenerate modes were found to be extended in nature. Furthermore, the extended nondegenerate modes were found to exist side by side with the superlocalized persistent degenerate modes. This result is unlike that of a disordered system where one would find a single demarcation frequency separating the extended states from the localized states.

One of the purposes of this paper is to investigate in detail the role of the boundary condition on various aspects of the vibrational dynamics of the Vicsek fractal. Also, we use a somewhat different treatment from our earlier paper[9] so that the interplay among the local symmetry, the self-similarity, the loopless structure, and the boundary condition on the nature of the frequency spectrum can be appreciated readily. The key lies in expressing the dynamical matrix properly where all these effects can be incorporated simultaneously. In this new treatment, the conditions for the existence of persistent modes and the pattern of evolution of persistent degenerate modes emerge out very simply. Finally, the differences between the results for fixed-end and free-end boundary conditions also become very apparent. Some preliminary results of this calculation were reported elsewhere.[12]

In Sec. II, we present the structure of the dynamical matrix and investigate in detail the effects of local symmetry, self-similarity, and the boundary condition on the

dynamics of the Vicsek fractal. In Sec. II C, we present the conditions for the existence of the persistent modes, which also yield the rule governing the pattern of evolution of the degree of degeneracy of these modes. In Sec. III, the nature of the eigenvectors corresponding to persistent degenerate modes is given. Section IV presents an analytical formula that gives a simple way to count the number of distinguishable threefold and nondegenerate modes. This formula is central to the prediction of the pattern of the frequency spectrum of a fractal of any stage, since all the persistent modes of a given stage are descendants of either a threefold degenerate mode or a nondegenerate mode of one of the previous stages. Section V presents a method to compute the frequencies corresponding to nondegenerate and threefold degenerate modes of any stage. We also present an exact analytical formula for the intensities of the persistent degenerate modes as $n \to \infty$, using which the exact frequency spectrum can be calculated. Section VI contains the calculation of the spectral dimension of the Vicsek fractal. Finally, our results are summarized in Sec. VII.

II. LOOPLESS STRUCTURE, LOCAL SYMMETRY, SELF-SIMILARITY AND THE BOUNDARY CONDITION

A. Structure of the dynamical matrix

Figure 1 shows the first and second stages of the Vicsek fractal. The nth stage Vicsek fractal can be constructed by connecting five $(n-1)$th-stage fractals. The construction follows the pattern such that one of the $(n-1)$th-stage components (clusters) serves as the central component of the nth-stage fractal, while the other four $(n-1)$th-stage components are connected only to the central component (cluster). The dynamical matrix of the nth-stage fractal describing the transverse vibrations with nearest-neighbor interactions can then be written as

$$\mathbf{H}_n = \begin{bmatrix} \mathbf{H}_{n-1}^c & \mathbf{V} & \mathbf{V} & \mathbf{V} & \mathbf{V} \\ \mathbf{V}^T & \mathbf{H}_{n-1}^s & 0 & 0 & 0 \\ \mathbf{V}^T & 0 & \mathbf{H}_{n-1}^s & 0 & 0 \\ \mathbf{V}^T & 0 & 0 & \mathbf{H}_{n-1}^s & 0 \\ \mathbf{V}^T & 0 & 0 & 0 & \mathbf{H}_{n-1}^s \end{bmatrix}, \quad (1)$$
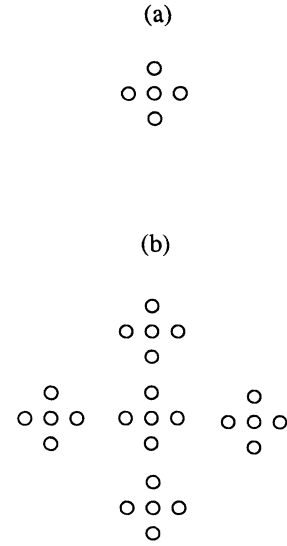

(a)

(b)

FIG. 1. First and second stages of the Vicsek fractal with the free-end boundary condition.

where $\mathbf{H}_{n-1}^c$ (the dynamical matrix of the central component) and $\mathbf{H}_{n-1}^s$ (the dynamical matrix of the side component) may differ slightly from $\mathbf{H}_{n-1}$, the dynamical matrix of the $(n-1)$th-stage fractal, due to the connections. The matrix $\mathbf{V}$ describes the interaction between the central cluster and one of the side clusters. It has only one nonvanishing element corresponding to the interaction between the site in the central cluster and the site in the side cluster. In partitioning the dynamical matrix $\mathbf{H}_n$ in the form as given in Eq. (1), we are emphasizing the self-similarity, i.e., the nth-stage fractal is constructed by assembling five copies of the $(n-1)$th-stage fractal. The dimensions of the matrices describing $\mathbf{H}_{n-1}^c$ and the four identical $\mathbf{H}_{n-1}^s$'s are $N_{n-1} = 5^{n-1}$, the same as the dimension of the dynamical matrix $\mathbf{H}_{n-1}$ of the $(n-1)$th-stage fractal.

In the case of the free-end boundary condition, the dynamical matrix of the first stage Vicsek fractal is given by

$$\mathbf{H}_1 = \begin{bmatrix} 4\gamma/m & -\gamma/m & -\gamma/m & -\gamma/m & -\gamma/m & -\gamma/m \\ -\gamma/m & \gamma/m & 0 & 0 & 0 & 0 \\ -\gamma/m & 0 & \gamma/m & 0 & 0 & 0 \\ -\gamma/m & 0 & 0 & \gamma/m & \gamma/m & 0 \\ -\gamma/m & 0 & 0 & 0 & 0 & \gamma/m \end{bmatrix}, \quad (2)$$

where γ is the force constant and m is the mass of the particle. The dynamical matrix of the second stage can then be constructed according to Eq. (1) as

$$H_2 = \begin{bmatrix} H_1^c & V & V & V & V \\ V^T & H_1^s & 0 & 0 & 0 \\ V^T & 0 & H_1^s & 0 & 0 \\ V^T & 0 & 0 & H_1^s & 0 \\ V^T & 0 & 0 & 0 & H_1^s \end{bmatrix} \tag{3}$$

with

$$H_1^c = \begin{bmatrix} 4 & -1 & -1 & -1 & -1 \\ -1 & 2 & 0 & 0 & 0 \\ -1 & 0 & 2 & 0 & 0 \\ -1 & 0 & 0 & 2 & 0 \\ -1 & 0 & 0 & 0 & 2 \end{bmatrix} \tag{4}$$

and

$$H_1^s = \begin{bmatrix} 4 & -1 & -1 & -1 & -1 \\ -1 & 2 & 0 & 0 & 0 \\ -1 & 0 & 1 & 0 & 0 \\ -1 & 0 & 0 & 1 & 0 \\ -1 & 0 & 0 & 0 & 1 \end{bmatrix} . \tag{5}$$

In writing down Eqs. (4) and (5), the dynamical matrices have been expressed in the reduced unit of $\gamma/m = 1$. A comparison of Eq. (2) with Eqs. (4) and (5) shows that H_1^c differs from H_1 only in the diagonal elements corresponding to the four sites in the central cluster directly connected to the four side clusters. Similarly, H_1^s is seen to be different from H_1 only in one diagonal element associated with the site, which connects the side cluster in question directly to the central cluster. In general, one can write

$$H_{n-1}^c = H_{n-1} + H_{n-1}' \tag{6}$$

and

$$H_{n-1}^s = H_{n-1} + H_{n-1}'' , \tag{7}$$

where H_{n-1}' is a matrix of the same dimension as H_{n-1} but with only four nonvanishing elements, which are along the diagonal and are associated with the four sites in the central cluster connected directly to the side clusters and H_{n-1}'' is a matrix with only one nonvanishing element, which is along the diagonal and is associated with the site in the side cluster in question connecting directly to the central cluster. The magnitudes of these elements are all equal to 1 in the reduced unit of $\gamma/m = 1$. Equations (6) and (7) contain the boundary effect imposed on the fractal. For example, in the case of the fixed-end boundary condition $H_{n-1}' = H_{n-1}'' = 0$, while in the case of the free-end boundary condition $H_{n-1}' = H_{n-1}'' \neq 0$. In fact, expressing the dynamical matrix as given in Eq. (1), together with Eqs. (6) and (7), can bring out clearly the interplay among all the factors such as the treelike structure, the local symmetry, the self-similarity and the boundary condition on the vibrational dynamics of a Vicsek fractal.

B. Local symmetry

In this section, we highlight only the interplay between the local symmetry and the structure of the fractal, which leads to an important classification of the degenerate and nondegenerate modes. For this purpose, it is more convenient to rewrite the dynamical matrix H_n of the nth-stage fractal as

$$H_n = \begin{bmatrix} h_c & \tilde{V} & \tilde{V} & \tilde{V} & \tilde{V} \\ \tilde{V}^T & \tilde{H}_n & 0 & 0 & 0 \\ \tilde{V}^T & 0 & \tilde{H}_n & 0 & 0 \\ \tilde{V}^T & 0 & 0 & \tilde{H}_n & 0 \\ \tilde{V}^T & 0 & 0 & 0 & \tilde{H}_n \end{bmatrix} , \tag{8}$$

where $h_c = 4$ is a scalar quantity describing the particle at the central site, $\tilde{H}_n$ the dynamical matrix of one of the four equivalent side branches surrounding the central site, and $\tilde{V}$ the matrix giving the interaction of the central site with one of the side branches. The dimension of the matrix describing each side branch, $\tilde{H}_n$, is $\frac{1}{4}(N_n - 1)$. The situation can be best illustrated by the drawing in Fig. 2 where an nth-stage fractal is shown. The subsystems shown in the central and outer square boxes describe the $(n-1)$th-state clusters and their corresponding system matrices are given by H_{n-1}^c and H_{n-1}^s, respectively. On the other hand, the subsystem shown in the elliptical box outlined by the broken line is one of the four equivalent branches of the nth-stage fractal with its system matrix described by $\tilde{H}_n$. Thus the nth-stage fractal
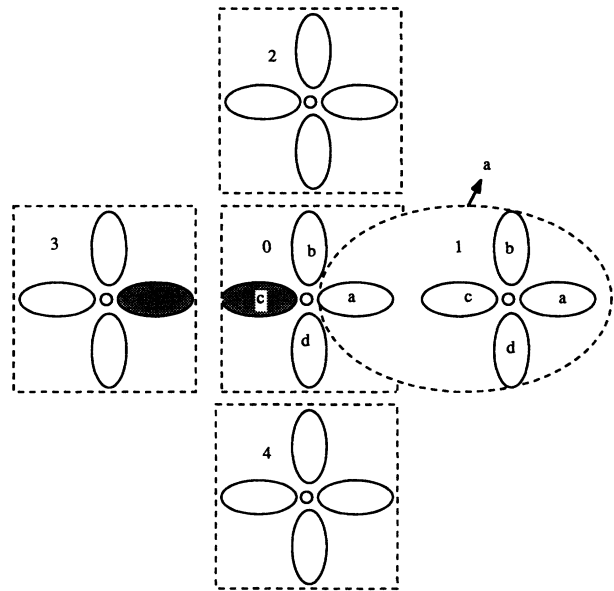

FIG. 2. A schematic representation of the nth-stage fractal in terms of the nth-stage clusters. The subsystem shown inside the ellipse, highlighted by the broken line, is one of the four equivalent side branches of the nth-stage fractal. The matrix describing these side branches is depicted in the text as $\tilde{H}_n$. Two of the branches of the $(n-1)$th-state clusters are highlighted to facilitate the discussions in the text.

can be viewed as having a treelike structure with four equivalent side branches (broken ellipse) connected via the central site. Similarly, the $(n-1)$th-stage cluster consists of four equivalent side branches (solid ellipses) connected at its central site. The self-similar nature of the fractal at successive stages can be seen by the equivalence in the structures of the successive stages, which is also reflected by the equivalence in the structures of the branches associated with successive stages.

The eigenvalue problem of the nth stage, $(\mathbf{H}_n - \omega^2 \mathbf{I}_n)\mathbf{u}_n = 0$, can be written as

$$(4 - \omega^2)u_n^c + \widetilde{\mathbf{V}}\widetilde{\mathbf{u}}_n(a) + \widetilde{\mathbf{V}}\widetilde{\mathbf{u}}_n(b) + \widetilde{\mathbf{V}}\widetilde{\mathbf{u}}_n(c) + \widetilde{\mathbf{V}}\widetilde{\mathbf{u}}_n(d) = 0 ,$$

$$(9)$$

$$(\widetilde{\mathbf{H}}_n - \omega^2 \widetilde{\mathbf{I}}_n)\widetilde{\mathbf{u}}_n(\alpha) + \widetilde{\mathbf{V}}^T u_n^c = 0 \quad (\alpha = a,b,c,d) , \quad (10)$$

where the eigenvector $\mathbf{u}_n$ describing the displacement field of the nth-stage fractal is broken down into

$$\mathbf{u}_n^T = (u_n^c, \widetilde{\mathbf{u}}_n^T(a), \widetilde{\mathbf{u}}_n^T(b), \widetilde{\mathbf{u}}_n^T(c), \widetilde{\mathbf{u}}_n^T(d)) \quad (11)$$

with u_n^c being the displacement at the central site, and $\widetilde{\mathbf{u}}_n(\alpha)$ the displacement field of the side branch α $(\alpha = a,b,c,d)$ surrounding the central site.

Consider the case when ω_i is an eigenfrequency of $\mathbf{H}_n$ with $u_n^c = k \neq 0$. Then Eq. (10) will yield

$$\widetilde{\mathbf{u}}_n(\alpha) = -[(\widetilde{\mathbf{H}}_n - \omega_i^2 \widetilde{\mathbf{I}}_n)^{-1}\widetilde{\mathbf{V}}^T]k = \mathbf{A} \quad (\alpha = a,b,c,d) .$$

$$(12)$$

According to Eq. (11), the eigenvector corresponding to ω_i must be

$$\mathbf{u}_n^T = (k, \mathbf{A}^T, \mathbf{A}^T, \mathbf{A}^T, \mathbf{A}^T) . \quad (13)$$

Since $\mathbf{A}$ is proportional to k [see Eq. (12)], $\mathbf{u}_n$ is therefore proportional to k. Hence, $\mathbf{u}_n$ is unique up to a constant factor k. The eigenfrequency ω_i must be a nondegenerate mode. If, on the other hand, $u_n^c = 0$, then Eq. (10) requires

$$(\widetilde{\mathbf{H}}_n - \omega_i^2 \widetilde{\mathbf{I}}_n)\widetilde{\mathbf{u}}_n(\alpha) = 0 \quad \text{for } \alpha = a,b,c,d , \quad (14)$$

and Eq. (9) reduces to a scalar equation,

$$\widetilde{u}_n(a,1) + \widetilde{u}_n(b,1) + \widetilde{u}_n(c,1) + \widetilde{u}_n(d,1) = 0 , \quad (15)$$

where $\widetilde{u}_n(\alpha,1)$ is the displacement at the site in the branch α adjacent to and directly connected with the central site. From Eqs. (11) and (14), a nontrivial solution for $\mathbf{u}_n$ requires that ω_i must also be an eigenfrequency of $\widetilde{\mathbf{H}}_n$. Since $\widetilde{\mathbf{u}}_n(\alpha)$ $(\alpha = a,b,c,d)$ satisfies Eq. (14) with

only one condition [Eq. (15)] relating them, Eq. (11) then indicates that there can be many possible eigenvectors $\mathbf{u}_n$ when these four fields are combined to form the eigenvector corresponding to ω_i. Hence, ω_i must be a degenerate mode of $\mathbf{H}_n$. Thus, if ω_i is a degenerate mode of $\mathbf{H}_n$, u_n^c must vanish, and ω_i must also be an eigenmode of $\widetilde{\mathbf{H}}_n$.

The simplest degenerate mode of $\mathbf{H}_n$ is when ω_i happens to be a nondegenerate mode of $\widetilde{\mathbf{H}}_n$. In this case, the four displacement fields $\widetilde{\mathbf{u}}_n(\alpha)$ $[(\alpha = a,b,c,d)]$ must be proportional to each other because they all represent eigenvectors to the same nondegenerate eigenvalue. However, with the relation Eq. (15) among these four fields, there can be only three independent solutions when they are combined to form the eigenvector $\mathbf{u}_n$ for $\mathbf{H}_n$ according to Eq. (11). Hence ω_i is a threefold degenerate mode of $\mathbf{H}_n$ when it is also a nondegenerate mode of $\widetilde{\mathbf{H}}_n$.

The analysis presented above depends only on the structure of the dynamical matrix and the local symmetry, not on the details of the dynamical matrix. Therefore, the conclusion drawn in this section is independent of the boundary condition.

C. Boundary condition

In this section we highlight the effect of the boundary condition on the origin, nature, and the evolution of persistent modes. As pointed out earlier, this can be best accomplished by partitioning the matrix in the form given by Eq. (1), where the interplay among the local symmetry, the self-similarity, the treelike structure, and the boundary condition can be readily treated.

Let ω_i be an eigenfrequency of $\mathbf{H}_{n-1}$ so that

$$(\mathbf{H}_{n-1} - \omega_i^2 \mathbf{I}_{n-1})\mathbf{u}_{n-1} = 0 \quad (16)$$

Consider the operation $(\mathbf{H}_n - \omega_i^2 \mathbf{I}_n)\mathbf{u}_n$ where $\mathbf{u}_n$ is a displacement field of the nth stage fractal. The vector $\mathbf{u}_n$ can be expressed as

$$\mathbf{u}_n^T = (\mathbf{u}_{n-1}^T(0), \mathbf{u}_{n-1}^T(1), \mathbf{u}_{n-1}^T(2), \mathbf{u}_{n-1}^T(3), \mathbf{u}_{n-1}^T(4)) ,$$

$$(17)$$

where $\mathbf{u}_{n-1}(k)$ is the displacement field of the kth component cluster $(k = 0-4)$, with $k = 0$ denoting the central $(n-1)$th-stage cluster. It should be noted that in Eq. (17) the displacement field of the nth-stage fractal is expressed in terms of the displacement fields of component clusters $[\mathbf{u}_{n-1}(k), \quad k = 0,1,2,3,4]$ rather than component branches $[\widetilde{\mathbf{u}}_n(\alpha), \quad \alpha = a,b,c,d]$. Using Eqs. (1), (6), and (7), we can write

$$(\mathbf{H}_n - \omega^2 \mathbf{I}_n)\mathbf{u}_n = \begin{bmatrix} (\mathbf{H}_{n-1} - \omega_i^2 \mathbf{I}_{n-1})\mathbf{u}_{n-1}(0) + \mathbf{H}_{n-1}'\mathbf{u}_{n-1}(0) + \sum_{k=1}^{4} \mathbf{V}\mathbf{u}_{n-1}(k) \\ \mathbf{V}^T\mathbf{u}_{n-1}(0) + \mathbf{H}_{n-1}''\mathbf{u}_{n-1}(1) + (\mathbf{H}_{n-1} - \omega_i^2 \mathbf{I}_{n-1})\mathbf{u}_{n-1}(1) \\ \vdots \\ \mathbf{V}^T\mathbf{u}_{n-1}(0) + \mathbf{H}_{n-1}''\mathbf{u}_{n-1}(4) + (\mathbf{H}_{n-1} - \omega_i^2 \mathbf{I}_{n-1})\mathbf{u}_{n-1}(4) \end{bmatrix} . \quad (18)$$

The structures of $\mathbf{H}'_{n-1}$, $\mathbf{H}''_{n-1}$, and $\mathbf{V}$'s, are such that the column vector $\mathbf{H}'_{n-1}\mathbf{u}_{n-1}(0)+\sum_{k=1}^{4}\mathbf{V}\mathbf{u}_{n-1}(k)$ has only four nonvanishing elements $u_{n-1}(0,k)-u_{n-1}(k,1)$ ($k=1,2,3,4$), while the column vector $\mathbf{V}^T\mathbf{u}_{n-1}(0)$ $+\mathbf{H}''_{n-1}\mathbf{u}_{n-1}(k)$ has only one nonvanishing element $-u_{n-1}(0,k)+u_{n-1}(k,1)$. Here $u_{n-1}(0,k)$, $k=1,2,3,4$, denotes the displacement of the site in the central cluster adjacent to the kth side cluster and $u_{n-1}(k,1)$ the displacement of the site in kth side cluster adjacent to the central cluster. From Eqs. (16) and (18), it can be seen that, if $\mathbf{u}_{n-1}(k)$ ($k=0,1,2,3,4$) is an eigenvector of $\mathbf{H}_{n-1}$ corresponding to the eigenfrequency ω_i, and if the condition

$$u_{n-1}(0,k)=u_{n-1}(k,1) \quad (k=1,2,3,4) \tag{19}$$

is satisfied, then

$$(\mathbf{H}_n-\omega_i^2\mathbf{I}_n)\mathbf{u}_n=0 . \tag{20}$$

In other words, an eigenfrequency ω_i of H_{n-1}, be it a degenerate mode (as in the case of fixed-end boundary condition[9]) or a nondegenerate mode, will persist and become an eigenfrequency of $\mathbf{H}_n$ with its eigenvector $\mathbf{u}_n$ given by Eq. (17). The components of $\mathbf{u}_n$, namely, $\mathbf{u}_{n-1}(k)$ ($k=0,\dots,4$), are eigenvectors of $\mathbf{H}_{n-1}$ corresponding to the same eigenfrequency ω_i subject to the conditions given by Eq. (19). The persistence of a nondegenerate mode from one stage to the next is a new feature due to the free-end boundary condition. It is not found in the case with fixed-end boundary condition.[8-10]

When five copies of the $(n-1)$th-stage clusters are assembled to form the nth-stage fractal, the above discussion indicates that every eigenmode ω_i of $\mathbf{H}_{n-1}$ will persist and be an eigenmode of $\mathbf{H}_n$ subject to the four conditions given by Eq. (19). Hence if $\mathbf{D}_{n-1}$ is the degree of degeneracy of an eigenmode ω_i of $\mathbf{H}_{n-1}$, then this mode will be an eigenmode of $\mathbf{H}_n$ with a degree of degeneracy $\mathbf{D}_n$ given by

$$\mathbf{D}_n=5\mathbf{D}_{n-1}-4 . \tag{21}$$

In particular, if the mode is nondegenerate in a given stage, it will persist as a nondegenerate mode in the subsequent stages. On the other hand, since the lowest degree of degeneracy of a degenerate mode is three, the path of evolution of the degree of degeneracy of a degenerate mode will follow the pattern: 3,11,51,251,. . . .

The analysis given in this section is based on the structure, local symmetry, the self-similarity of the Vicsek fractal and the boundary condition imposed on it. The conclusion is therefore a consequence of the interplay among these factors. The effect of the free-end boundary condition is, however, clearly demonstrated by the relation given in Eq. (19). It determines the persistency of an eigenfrequency from one stage to the next. It also controls the pattern of evolution of the degree of degeneracy of a persistent mode [see Eq. (21)]. Hence the role played by the boundary condition is reflected in the relation defining the linkage between the central cluster and the side clusters [Eq. (19) for the free-end case] as five copies of the $(n-1)$th-stage cluster are assembled to form the nth-stage fractal.

In the case of the fixed-end boundary condition, since $\mathbf{H}'_{n-1}=\mathbf{H}''_{n-1}=0$, the condition for the persistent mode to appear requires $u_{n-1}(0,k)=0$ and $u_{n-1}(k,1)=0$ ($k=1,2,3,4$). In this case, when the persistent mode of degree of degeneracy $\mathbf{D}_{n-1}$ evolves into the next stage, it will be subjected to eight conditions. Hence, the degree of degeneracy of the mode in the nth stage will be governed by $\mathbf{D}_n=5\mathbf{D}_{n-1}-8$. This result was proved earlier [Ref. 9, Eq. (25)] using a different treatment. The evolution of the degree of degeneracy of the degenerate mode in this case will follow the pattern 3,8,32,152. . ., and so on.

III. THE NATURE OF THE PERSISTENT MODES

A. Persistent nondegenerate modes

Let ω_i be a nondegenerate mode of $\mathbf{H}_{n-1}$. When this mode persists into the nth stage, the component fields $\mathbf{u}_{n-1}(k)$ ($k=0,\dots,4$), must all be eigenvectors corresponding to the nondegenerate mode ω_i of $\mathbf{H}_{n-1}$ [see Eq. (16)]. Hence, they can differ only by multiplicative factors. Using the condition given by Eq. (19), the factor between any two of the eigenvectors must be one. Hence, we obtain

$$\mathbf{u}_{n-1}(0)=\mathbf{u}_{n-1}(1)=\mathbf{u}_{n-1}(2)=\mathbf{u}_{n-1}(3)=\mathbf{u}_{n-1}(4) . \tag{22}$$

According to Eqs. (17) and (22), when a nondegenerate mode of $\mathbf{H}_{n-1}$ persists and becomes a nondegenerate mode of $\mathbf{H}_n$, the eigenvector $\mathbf{u}_n$ will be a perfect patchup of five identical eigenvectors of $\mathbf{u}_{n-1}(k)$ of the five component clusters of the $(n-1)$th-stage. The mode in question must therefore be an extended mode.

B. The persistent degenerate mode

Let ω_i be a threefold degenerate mode of $\mathbf{H}_{n-1}$ so that it is also a nondegenerate mode of $\tilde{\mathbf{H}}_{n-1}$. The eigenvector $\mathbf{u}_{n-1}$ for any degenerate mode can be written as

$$\mathbf{u}_{n-1}^T=(0,\tilde{\mathbf{u}}_{n-1}^T(a),\tilde{\mathbf{u}}_{n-1}^T(b),\tilde{\mathbf{u}}_{n-1}^T(c),\tilde{\mathbf{u}}_{n-1}^T(d)) ,$$

where the displacement of the central site is zero and $\tilde{\mathbf{u}}_{n-1}(\alpha)$ is the displacement field of the branch α. Because $\tilde{\mathbf{u}}_{n-1}(\alpha)$'s ($\alpha=a,b,c,d$) are all eigenvectors corresponding to the nondegenerate mode ω_i of $\tilde{\mathbf{H}}_{n-1}$, they must be proportional to each other. The constants of proportionality among them are determined by the scalar equation

$$\tilde{u}_{n-1}(a,1)+\tilde{u}_{n-1}(b,1)+\tilde{u}_{n-1}(c,1)+\tilde{u}_{n-1}(d,1)=0 . \tag{23}$$

Because of the equivalence of the four branches, a logical choice will be to assign

$$\tilde{u}_{n-1}(a,1)=\tilde{u}_{n-1}(b,1)=\tilde{u}_{n-1}(c,1)=-1 . \tag{24}$$

Equation (23) then dictates that

$$\tilde{u}_{n-1}(d,1)=3 . \tag{25}$$

The ratio of the constants of proportionality among the four branches is therefore

$$|\bar{u}_{n-1}(a)|:|\bar{u}_{n-1}(b)|:|\bar{u}_{n-1}(c)|:|\bar{u}_{n-1}(d)|=1:1:1:3 \ .$$

Thus the eigenvector of a threefold degenerate mode must consist of three identical patterns in any three of the four equivalent branches and a prominent hump of the same pattern in the fourth branch. The pattern of the prominent hump is every way the same as the pattern in the other three branches except its magnitude is enhanced by a factor of three.

When the threefold degenerate mode of H_{n-1} persists into the nth-stage as an 11-fold degenerate mode, the condition given in Eq. (19), which is the condition for the persistency of the mode establishes a relation of linkage between the two bordering branches, one in the central cluster and the other in the side cluster. Because ω_i is a nondegenerate mode of $\tilde{H}_{n-1}$, Eq. (19) then requires

$$\bar{u}_{n-1}(0,\alpha_0)=\bar{u}_{n-1}(k,\alpha_k) \quad (k=1,\ldots,4) \ , \tag{26}$$

where $\bar{u}_{n-1}(0,\alpha_0)$ denotes the displacement field of the α_0 branch of the central (0) cluster and $\bar{u}_{n-1}(k,\alpha_k)$ is the displacement field of the α_k branch of the kth cluster adjacent to the α_0 branch. The relation (26) in fact provides two possibilities for linkage between any two bordering clusters: (i) If the prominent hump of the original threefold mode in one of the cluster is in the region of linkage, Eq. (26) requires that the prominent hump of the cluster, which is linked to the cluster in question must also be in the region of linkage. This alignment then gives rise to a resonant mode at the bridging location corresponding to the region of linkage. This is a new feature associated with the free-end boundary condition. It is not found in the case of the fixed-end boundary condition. (ii) If none of the prominent humps of the bordering clusters is in the region of linkage, Eq. (26) simply provides the link for the persistent mode to extend from the prominent hump to the rest of the system.

The condition of linkage given by Eq. (26), together with Eq. (23), controls the magnitude of displacements of the outward branches (unshaded lobes in Fig. 2). These conditions introduce a reduction in the magnitudes of the displacement fields of the three outward branches with respect to the branch that is already linked (shaded lobes in Fig. 2). However, the reduction does not distort the signature of the original threefold mode, which is carried by all the component fields $\bar{u}_{n-1}(k,\alpha)$. As the fractal evolves from one stage to the next, new links will be formed and at each stage the magnitude of displacement fields of the outward branches will be less than the previous stage, leading to the superlocalization of the persistent mode.

Two eigenvectors corresponding to a persistent degenerate mode of the third stage are illustrated in Figs. 3(a) and 3(b), respectively. The eigenfrequency of the mode shown is $\omega^2=1.0$. This mode occurs in the first stage as a threefold degenerate mode and it evolves into a 51-fold degenerate mode in the third stage. The eigenvector shown in Fig. 3(a) is a resonant mode at the bridging location, which, although a superlocalized mode, is not
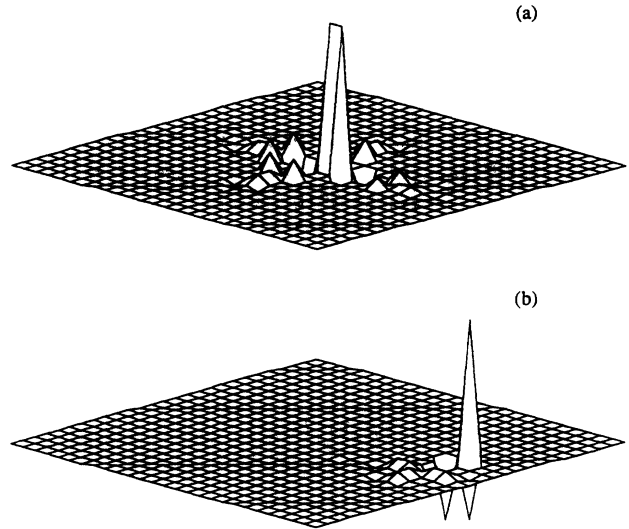

FIG. 3. Two types of eigenvectors corresponding to a persistent degenerate mode ($\omega^2=1.0$) of the third state Vicsek fractal with free-end boundary condition is illustrated. (a) shows a resonating bridge-localized mode, while (b) shows an edge-confined superlocalized mode.

found in the case of the fixed-end boundary condition.[9,10] The superlocalized mode shown in Fig. 3(b) is similar to the ones found in the case of the fixed-end boundary condition. Figures 4(a) and 4(b) show eigenvectors corresponding to nondegenerate modes. In Fig. 4(a), a nondegenerate mode ($\omega^2=5.41$) that appears for the first time
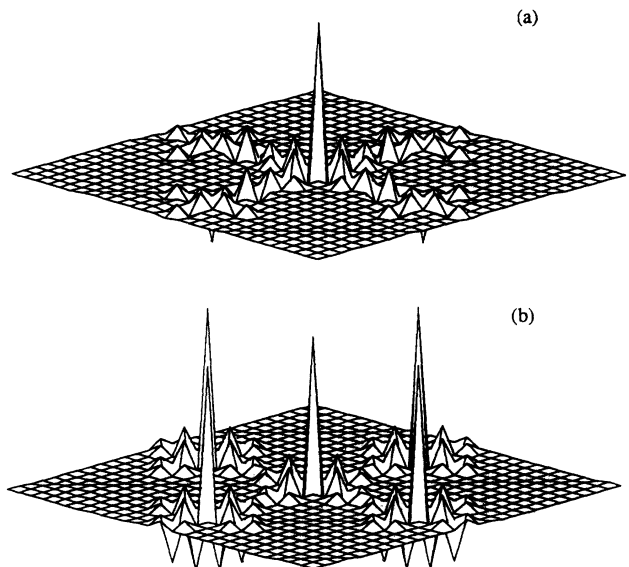

FIG. 4. Eigenvectors corresponding to two selected nondegenerate modes of the third-stage Vicsek fractal with free-end boundary condition. (a) shows the eigenvector corresponding to the nondegenerate mode at $\omega^2=5.41$, which appears for the first time in the third stage, while (b) shows a persistent nondegenerate mode at $\omega^2=5.38$ that was also found in the second stage. The eigenvector in (b) is a perfect patchup of five identical eigenvectors of the previous stage. In both cases (a) and (b) the eigenvector is an extended mode.

DYNAMICS OF A VICSEK FRACTAL: THE BOUNDARY ...

in the third stage is shown, while Fig. 4(b) shows a persistent nondegenerate mode ($\omega^2 = 5.38$) that occurred in the second stage also. It can be seen that the nondegenerate modes are all extended.

IV. NUMBER OF DISTINGUISHABLE NONDEGENERATE AND THREEFOLD DEGENERATE MODES

From the discussion in Secs. II and III, it can be seen that the frequency spectrum of an nth-stage fractal with the free-end boundary condition is also composed of both nondegenerate and degenerate modes, just like the case with the fixed-end boundary condition. The nondegenerate component, however, consists of both persistent nondegenerate modes from previous stages satisfying the condition of persistency given by Eq. (19) and additional nondegenerate modes, which are not present in the previous stages and do not satisfy Eq. (19). The degenerate component consists of D_1-fold, D_2-fold, etc., and D_n-fold degenerate modes with $D_n = 5D_{n-1} - 4$ and $D_1 = 3$. The D_2-fold, D_3-fold, etc., and D_n-fold degenerate modes are persistent modes evolved from the threefold degenerate modes of previous stages. For example, a D_n-fold degenerate mode exists as a threefold degenerate mode in the first stage, and is present in the subsequent stages as D_2-fold, D_3-fold, etc., and D_{n-1}-fold degenerate mode, respectively. Thus, to determine the complete frequency spectrum of the nth-stage fractal, one only needs to determine the nondegenerate modes and the threefold degenerate modes.

Let $d_3(n)$ be the number of threefold degenerate modes of the nth stage. Since the threefold degenerate mode of $\mathbf{H}_n$ is also a nondegenerate mode of $\tilde{\mathbf{H}}_n$, we have[13]

$$d_3(n) = \tfrac{1}{4}\{(N_n - 1) - [d_3(1) \times (D_n + 1)$$
$$+ \cdots + d_3(n-1) \times (D_2 + 1)]\} \ ,$$
(27)

where $N_n = 5^n$ is the number of particles in the nth stage. Using Eq. (27), it can be shown (see Appendix A) that $d_3(n)$ is given by the relation

$$d_3(n) = 3^{n-1} \ .$$
(28)

The number of nondegenerate modes of the nth-stage, $d_1(n)$, is accordingly given by

$$d_1(n) = N_n - \{d_3(1) \times D_n + \cdots + d_3(n) \times D_1\} \ . \quad (29)$$

Equation (29) can be further simplified (see Appendix B) to yield

$$d_1(n) = d_1(n-1) + d_3(n) \ .$$
(30)

Therefore, the number of additional nondegenerate modes in the nth-stage $[d_1(n) - d_1(n-1)]$, which are not present in the previous stages is the same as $d_3(n)$, the number of threefold degenerate modes of the nth stage.

V. FREQUENCY SPECTRUM

The eigenfrequencies of the Vicsek fractal of a given stage are completely determined once the eigenfrequencies corresponding to the additional nondegenerate modes and the threefold degenerate modes are calculated. This task can be accomplished by following the same renormalization procedure as given in the Ref. 10.

The equation of motion for the transverse vibrations of the first stage Vicsek fractal with the free-end boundary condition can be expressed as

$$(4 - \omega^2)u - \sum_\alpha v_\alpha = 0 \ ,$$
(31)

$$(1 - \omega^2)v_\alpha - u = 0 \quad (\alpha = a, b, c, d) \ ,$$
(32)

where u is the displacement at the central site and v_α's are the displacements of the four outer sites. The equations of motion of the second stage Vicsek fractal can be reduced into those of a five-particle system with renormalized force constants linking the central site and the four central sites of the outer clusters. The equation of motion for the second stage is then given by

$$(4 - \alpha_2)u - \kappa_2 \sum_\alpha v_\alpha = 0 \ ,$$
(33)

$$(4 - \beta_2)v_\alpha - \kappa_2 u = 0 \quad (\alpha = a, b, c, d) \ ,$$
(34)

where we again designate by u the displacement at the central site and by v_α's the displacements at the central sites of the outer clusters. In Eqs. (33) and (34), we have

$$\alpha_2 = \omega^2 + \frac{4(2 - \omega^2)}{(1 - \omega)^2(3 - \omega^2)} \ ,$$
(35)

$$\beta_2 = \omega^2 + \frac{3}{(1 - \omega^2)} + \frac{(2 - \omega^2)}{(1 - \omega^2)(3 - \omega^2)} \ ,$$
(36)

$$\kappa_2 = \frac{1}{(1 - \omega^2)(3 - \omega^2)} \ .$$
(37)

The renormalized equations of motion connecting the displacement of the central site (u) and the central sites of the outer clusters (v_α's) of the nth stage with $n \geq 3$ can be obtained by a similar procedure. This leads to the following sets of equations.

$$(4 - \alpha_n)u = \kappa_n \sum_\alpha v_\alpha = 0 \ ,$$
(38)

$$(4 - \beta_n)v_\alpha - \kappa_n u = 0 \quad (\alpha = a, b, c, d)$$
(39)

with

$$\alpha_n = \alpha_{n-1} + \frac{4\kappa_{n-1}^2(4 - \tilde{\beta}_{n-1})}{(4 - \tilde{\beta}_{n-1})^2 - \kappa_{n-1}^2} \ ,$$
(40)

$$\beta_n = \alpha_{n-1} + \frac{3\kappa_{n-1}^2}{4 - \beta_{n-1}} + \frac{\kappa_{n-1}^2(4 - \tilde{\beta}_{n-1})}{(4 - \tilde{\beta}_{n-1})^2 - \kappa_{n-1}^2} \ ,$$
(41)

$$\tilde{\beta}_n = \alpha_{n-1} + \frac{2\kappa_{n-1}^2}{4 - \beta_{n-1}} + \frac{2\kappa_{n-1}^2(4 - \tilde{\beta}_{n-1})}{(4 - \tilde{\beta}_{n-1})^2 - \kappa_{n-1}^2} \ ,$$
(42)

$$\tilde{\beta}_2 = \omega^2 + \frac{2}{1 - \omega^2} + \frac{2(2 - \omega^2)}{(1 - \omega^2)(3 - \omega^2)} \ ,$$
(43)

$$\kappa_n = \frac{\kappa_{n-1}^3}{(4-\bar{\beta}_{n-1})^2 - \kappa_{n-1}^2} \quad . \tag{44}$$

Since for a nondegenerate mode, $u \neq 0$ and $v_a = v_b = v_c = v_d$, Eqs. (38) and (39) can be combined to yield

$$\left[4 - \alpha_n - \frac{4\kappa_n^2}{4-\beta_n} \right] u = 0 \quad . \tag{45}$$

The fact that $u \neq 0$, therefore, leads to

$$f_n(\omega^2) = 4 - \alpha_n(\omega^2) - \frac{4\kappa_n^2(\omega^2)}{4-\beta_n(\omega^2)} = 0 \quad . \tag{46}$$

The roots of Eq. (46) are then the eigenfrequencies of the nondegenerate modes of the nth stage.

For a threefold degenerate mode, the condition $u = 0$ reduces Eq. (39) to

$$(4-\beta_n)v_\alpha = 0 \quad . \tag{47}$$

Since $v_\alpha \neq 0$, Eq. (47) then requires

$$4 - \beta_n(\omega^2) = 0 \quad . \tag{48}$$

Thus the roots of Eq. (48) give the eigenfrequencies of the threefold degenerate modes.

The nondegenerate and the threefold degenerate modes of a given stage of the Vicsek fractal with the free-end boundary condition can then be obtained as the roots of Eqs. (46) and (48), respectively. It should be noted that the parametric functions $\alpha_n(\omega^2)$, $\beta_n(\omega^2)$, and $\kappa_n(\omega^2)$ appearing in Eqs. (46) and (48) are computed recursively using Eqs. (40)–(46). This fact greatly facilitates the determination of the eigenfrequencies for the consecutive stages.

The frequency spectrum of the Vicsek fractal with free-end boundary condition as $n \to \infty$ can now be determined, since we know how to calculate the number of distinguishable degenerate modes of a given degeneracy (see Sec. IV) and their corresponding eigenfrequencies. The intensity of degenerate modes with the ith-highest degree of degeneracy is given by

$$I_i = D_{n-i+1}/N_n \quad , \tag{49}$$

where N_n is the number of particles in the system and D_n denotes the degree of degeneracy. Using Eq. (21) repeatedly, we obtain

$$D_{n-i+1} = 5^{n-i}(2+1/5^{n-i}) \quad . \tag{50}$$

Hence,

$$I_i = \frac{1}{5^i} \left[2 + \frac{1}{5^{n-i}} \right] \quad . \tag{51}$$

When $n \to \infty$, Eq. (51) reduces to

$$I_i = 2/5^i \quad \text{for } i \ll n \quad . \tag{52}$$

Using Eqs. (28), (46), (48), and (52), the frequency spectrum of the Vicsek fractal as $n \to \infty$ is constructed and shown in Fig. 5. It consists of a series of highly degen-
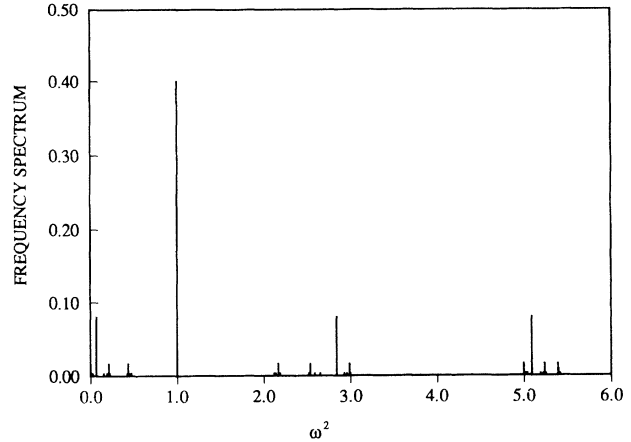

FIG. 5. The frequency spectrum of the Vicsek fractal with free-end boundary condition as $n \to \infty$.

erate atomiclike levels superimposed on a point dense, cantor set-like background spectrum. It is also a spectrum exhibiting the side-by-side coexistence of the super-localized modes and the extended modes, similar to the situation found in the case with a fixed-end boundary condition.[9,10] However, the detailed structure of the frequency spectrum is different from that of the fixed-end boundary condition.

VI. SPECTRAL DIMENSION

The spectral dimension of the Vicsek fractal with the free-end boundary condition can be determined using a scaling procedure suggested by Liu.[14] Let $\rho_n(\omega)$ be the frequency spectrum of the nth stage. Since the number of eigenmodes in a given interval $d\omega$ of the nth stage is compressed into an interval $d\omega'$ of the $(n+1)$th stage, we must have

$$\rho_n(\omega)d\omega = 5\rho_{n+1}(\omega')d\omega' \quad . \tag{53}$$

Denoting $\omega/\omega' = k$ and using the relation

$$\rho_n(\omega) \to A\omega^{\tilde{d}-1} \quad (\omega \to 0) \quad , \tag{54}$$

where $\tilde{d}$ is the spectral dimension, we obtain

$$\tilde{d} = \ln 5/\ln k \quad . \tag{55}$$

We have determined the spectral dimension by computing the ratio of the frequency intervals in the neighborhood of $\omega = 0$ of two consecutive stages, which contain the same number of eigenmodes. The value of k is obtained as the limit of the ratio when $n \to \infty$. It is found to have a value $\sqrt{15}$. The spectral dimension $\tilde{d}$ is therefore equal to

$$\tilde{d} = 2 \left/ \left[\frac{\ln 3}{\ln 5} + 1 \right] \right. \quad . \tag{56}$$

This result agrees with the universal relation between the fractal dimension $(\bar{d})$ and spectral dimension $(\tilde{d})$, namely, $\tilde{d} = 2\bar{d}/(\bar{d}+1)$, as given in Ref. 14.

In the case of the fixed-end boundary condition, one

can, in principle, define $\tilde{d}$ in the neighborhood of the fundamental frequency ω_0 (which is nonzero) using the relation $\rho(\omega)=(\omega-\omega_0)^{\tilde{d}-1}$. However, one has to ensure that the fixed value for ω_0 has been achieved to extract the correct numerical value for $\tilde{d}$ by considering larger and larger sized fractals. Because of this, it is numerically difficult to determine the exact value of the spectral dimension for the fixed-end boundary condition. However, our crude estimate indicates that the value of k corresponding to the fixed-end boundary condition is also in the neighborhood of $\sqrt{15}$, and hence $\tilde{d}$ is approximately the same as given in Eq. (56).

VII. SUMMARY

In this work, we have investigated in detail the role played by the boundary condition on various aspects of the dynamics of a Vicsek fractal by examining the interplay among the local symmetry, the self-similarity, and the loopless structure of the fractal. We found that the conditions for the occurrence of the persistent modes are different for the cases of the fixed-end and the free-end boundary conditions. Because of this, we find that both nondegenerate and degenerate modes are persistent in the case of free-end boundary condition, while only degenerate modes are persistent in the fixed-end boundary condition.[9] Furthermore, the nature and the pattern of evolution of the persistent degenerate modes are different in both cases. In the case of the free-end boundary condition, the persistent nondegenerate mode is a perfect patchup of five identical displacement fields corresponding to the parent nondegenerate mode. On the other hand, there are two types of persistent degenerate modes.

One of them is an edge-confined superlocalized mode as found in the case of fixed-end boundary case while the other is a bridge-localized resonant mode. In both cases, the frequency spectrum exhibits atomiclike levels superimposed on a point-dense background of the nondegenerate modes. Furthermore, in both cases, the extended and localized modes occur side-by-side in frequency unlike that of a disordered system. But, the detailed structures of the frequency spectrum are different for the two cases. Hence, the recursive structural rules as found in Ref. 11 for the hierarchies of isolated peaks are expected to be different for the free-end boundary case. In conclusion, we find that, although the general features of the frequency spectrum of a Vicsek fractal with the free-end boundary condition are similar to that of the case with the fixed-end boundary condition,[9,10] there are substantive differences. In fact, the signature of the boundary condition is found in almost every feature of the dynamics of a Vicsek fractal.

APPENDIX A

The eigenvalues of a first stage Vicsek fractal can be easily determined either from Eqs. (46) and (48) or by direct diagonlization. The five-mode spectrum consists of two nondegenerate modes at $\omega^2=0.0$ and 5.0 and a threefold degenerate mode at $\omega^2=1.0$. Hence $d_1(1)=2$ and $d_3(1)=1$. Using Eqs. (21) and (27), we obtain $d_3(2)=3^1$, $d_3(3)=3^2$, and so on. Let us assume that

$$d_3(k)=3^{k-1} . \tag{A1}$$

Equation (27) gives

$$d_3(k+1)=\tfrac{1}{4}\{(N_{k+1}-1)-[d_3(1)(D_{k+1}+1)+ \cdots +d_3(k-1)(D_3+1)+d_3(k)(D_2+1)]\} . \tag{A2}$$

Using the relations $N_{k+1}=5N_k$ and $D_n=5D_{n-1}-4$, Eq. (A2) can be rewritten as

$$d_3(k+1)=\tfrac{5}{4}\{(N_k-1)-[d_3(1)(D_k+1)+ \cdots +d_3(k-1)(D_2+1)]\}+1+2[d_3(1)+ \cdots d_3(k-1)]$$

$$-\tfrac{1}{4}(D_2+1)d_3(k) . \tag{A3}$$

Using Eqs. (21), (27), and (A1), we obtain

$$d_3(k+1)=5d_3(k)+1+3^{k-1}\left[1-\frac{1}{3^{k-1}}\right]-3d_3(k)=2d_3(k)+3^{k-1}=3^k . \tag{A4}$$

Hence, by the mathematical induction.

$$d_3(n)=3^{n-1} . \tag{A5}$$

APPENDIX B

From Eq. (29), we have

$$d_1(n)=N_n-\{d_3(1)\times D_n+ \cdots +d_3(n)\times D_1\} . \tag{B1}$$

Equation (B1) can be rewritten as

$$d_1(n)=\tfrac{1}{4}\times4\times(N_n-1)+1-\{\tfrac{1}{4}\times4d_3(1)(D_n+1)-d_3(1)+ \cdots +\tfrac{1}{4}\times4d_3(n-1)(D_2+1)-d_3(n-1)\}-d_3(n)\times D_1 .$$

Using Eq. (27), we obtain

$$d_1(n)=4d_3(n)-3d_3(n)+1+d_3(1)+ \cdots +d_3(n-1)=1+d_3(1)+ \cdots +d_3(n-1)+d_3(n)=d_1(n-1)+d_3(n) . \tag{B2}$$

[1] *Fractals in Physics,* edited by A. Aharony and J. Feder (North-Holland, Amsterdam, 1990).

[2] S. Alexander and R. Orbach, J. Phys. Lett. **43**, 625 (1982).

[3] I. Webman and G. S. Grest, Phys. Rev. B **31**, 1689 (1985).

[4] P. de Vries, H. de Raedt, and A. Lagendijk, Phys. Rev. B **62**, 2515 (1989).

[5] K. Yakubo and T. Wakayama, Phys. Rev. B **40**, 517 (1989).

[6] Y. E. Levy and B. Souillard, Europhys. Lett. **4**, 233 (1987).

[7] R. Rammal, J. Phys. **45**, 191 (1984).

[8] C. S. Jayanthi, S. Y. Wu, and J. Cocks, Phys. Rev. Lett. **69**, 1955 (1992).

[9] C. S. Jayanthi and S. Y. Wu, Phys. Rev. B **48**, 10 188 (1993).

[10] C. S. Jayanthi and S. Y. Wu, Phys. Rev. B **48**, 10 199 (1993).

[11] J. Q. You, C. H. Lam, F. Nori, and L. M. Sander, Phys. Rev. E **48**, R4183 (1993).

[12] C. S. Jayanthi and S. Y. Wu, Fractals **1**(3), 922 (1993).

[13] The quantity one is added to D_n to account for the condition of persistency as given by Eq. (19). Thus a D_n-fold degenerate mode of $\mathbf{H}_n$ with $n \geq 2$ contributes a degree of degeneracy of $\frac{1}{4}(D_n + 1)$ to $\tilde{\mathbf{H}}_n$.
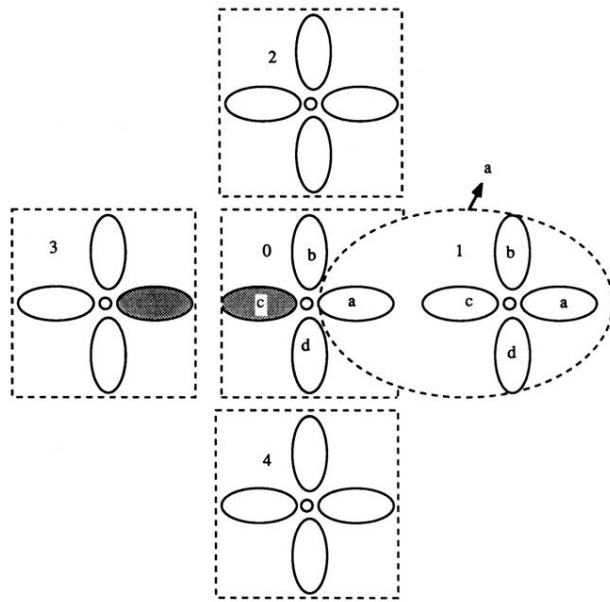
[14] S. H. Liu, Phys. Rev. B **30**, 4045 (1984).

FIG. 2. A schematic representation of the nth-stage fractal in terms of the nth-stage clusters. The subsystem shown inside the ellipse, highlighted by the broken line, is one of the four equivalent side branches of the nth-stage fractal. The matrix describing these side branches is depicted in the text as $\tilde{\mathbf{H}}_n$. Two of the branches of the $(n-1)$th-state clusters are highlighted to facilitate the discussions in the text.